Colloquium: Opportunities in nanomagnetism

S. D. Bader

Materials Science Division and Center for Nanoscale Materials, Argonne National Laboratory, Argonne, Illinois 60439, USA

(Published 3 January 2006)

Nanomagnetism is the discipline dealing with magnetic phenomena specific to structures having dimensions in the submicron range. This Colloquium addresses the challenges and scientific problems in this emerging area, including its fabrication strategies, and describes experiments that explore new spin-related behaviors in metallic systems as well as theoretical efforts to understand the observed phenomena. As a subfield of nanoscience, nanomagnetism shares many of the same basic organizing principles such as geometric confinement, physical proximity, and chemical self-organization. These principles are illustrated by means of several examples drawn from the quests for ultrastrong permanent magnets, ultra-high-density magnetic recording media, and nanobiomagnetic sensing strategies. As a final example showing the synergetic relationships to other fields of science, this Colloquium discusses the manipulation of viruses to fabricate magnetic nanoparticles.

DOI: 10.1103/RevModPhys.78.1 PACS number(s): 75.75.+a, 61.46.−w

CONTENTS

I. INTRODUCTION

A. History

Magnetism is one of the oldest scientific disciplines, but one also at the forefront of the emerging nanotechnology era. Figure 1 illustrates this interplay of the past and the present. On the left is a reproduction of a woodcut illustration from the book *De Magnete* written by William Gilbert and published in Latin in 1600. This book is regarded as the first to embrace the scientific method of inquiry. William Gilbert was a gentleman scientist whose day job was as a medical doctor, eventually as the personal physician to Queen Elizabeth I (Chapman, 1944). Juxtaposed to the right in Fig. 1 is a modern simulation of a magnetic vortex structure. The two images share the similarity of being circles that contain arrows. So what has changed in the 400+ years that have elapsed? The crucial difference is that Gilbert was concerned with geomagnetism; his image represents the planet Earth. The modern vortex structure to the right is for a submicron ferromagnetic dot. The difference in diameters is upwards of 14 orders of magnitude. Herein lies the advance: in the present work, we will be concerned with the opportunities associated with the nanoscale.

B. Challenges

The scientific quest in nanomagnetism can be framed quite succinctly. The goal is to (i) create, (ii) explore, and (iii) understand new nanomagnetic materials and phenomena. Throughout this paper, examples will be presented to highlight these three components of an integrated approach to nanomagnetism research. We create new materials via synthesis and fabrication routes. We explore them using major facilities such as synchrotron light sources, neutron scattering, and electron microscopies, as well as via bench-top and conventional

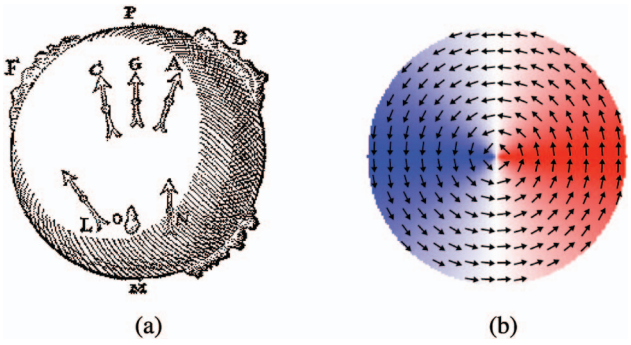

FIG. 1. (Color) Two pictures of circles with arrows inside: (a) from *De Magnete*, published in 1600 by William Gilbert. The image is a woodcut representation of the Earth, including a mountainous topology, in an effort to understand geomagnetism. (b) A generic modern micromagnetic simulation of a submicrometer magnetic vortex structure in Permalloy, such as is discussed by Novosad *et al.* (2002). It includes a central core where the spins point out of plane.

 ©2006 The American Physical Society

FIG. 2. (Color online) Grand challenges in nanomagnetism, emphasizing those related to strategic national goals, such as stimulating the economy, energy efficiency, homeland security, and defense. The underlying basic research needed involves creating new materials and understanding their spin-transport and spin dynamic properties.

laboratory facilities such as scanning probes, magnetometry, magneto-optics, and magnetotransport probes. To understand the materials we create, and the phenomena they exhibit, we rely on theory and simulation.

Figure 2 provides a sunburst representation of grand challenges in the field based on today's perspective. The important feature to keep in mind is that, while the challenges will be framed in terms of their relationships to societal benefits, the underlying basic science involves creating new materials and exploring and understanding issues in spin dynamics and spin transport. Starting at the top, we will go in clockwise fashion around the sunburst.

Ultrastrong Permanent Magnets. The first bubble is the quest for ultrastrong permanent magnets. This quest addresses the national need for energy efficiency, energy conservation, and energy self-sufficiency. The energy issue could very well be the most important challenge the world faces. Its implications are broad and pervasive. Nanoscience offers the possibility to create and deliver ultrastrong permanent magnets that could, for example, lead to more efficient and compact motors. Lighter weight motors could save fossil fuels in auto and air transportation, since motors are ubiquitous in these systems. Also, electric motors for hybrid automotive vehicles might become a major market soon.

Ultra-High-Density Media. Next, ultra-high-density media for magnetic recording is needed to reach the nation's goals for information storage. Today's media stores almost 100 Gbits/in.^{2}. In order to advance to Tbits/in.^{2} and beyond, new approaches are required, and nanomagnetism might provide what is needed. The field is presently at a crossroads, and will soon no longer be able to incrementally improve on a technology originally introduced in 1956. Thermal stability of small structures, as covered by Weller and Moser (1999), is one of the major issues. The design and scaling of sensitive read head sensors, based on the giant magnetoresistive effect, pose other major issues (Parkin *et al.*, 2003).

Spin Transistor with Gain. While the hard drive in one's laptop computer is a well-known component, the future might include additional magnetic subsystems. The basis for today's electronics is the semiconductor transistor [see Bardeen and Brattain (1948)], perfected over the years, which has replaced vacuum-tube technology. Semiconductor electronics utilize the *charge* of the electron flowing in its circuitry, but the electron also has a *spin*, the basis for magnetism. A spin transistor could add value to present-day electronics, as highlighted by Wolf *et al.* (2001), and as we will see in examples that follow. The challenge is not only to create a spin transistor, but also to realize one with gain. Creating a spin gain transistor that not only utilizes but amplifies the spin signal has presented so far insurmountable problems, as has been discussed by Nikonov and Bourianoff (2005), who propose a possible scheme. The fundamentals and applications within the field of magnetic electronics, or *spintronics*, have been reviewed by Zutic *et al.* (2004).

Nearly 100% Spin-Polarized Materials. To create a circuit where the flow of spins takes place, rather than, or in addition to, the flow of charge, requires nearly 100% spin-polarized materials. These can be found in exotic half-metallic ferromagnets, such as exist in some complex oxides and Heusler alloys (de Groot *et al.*, 1983). Half-metallic refers to the Fermi level intersecting the density of states within a gap for one spin subband but not the other.

Room-Temperature Magnetic Semiconductors. A related quest is for magnetic semiconductors, needed in order to interface the new functionalities of magnetic electronics to mainstream semiconductor circuitry (Ohno, 1998). Such magnetic semiconductors need to have their ferromagnetic ordering temperatures, or Curie temperatures, well above room temperature in order to integrate with existing technologies.

Instant Boot-Up Computer. One new spintronic device is the magnetic random access memory (MRAM) chip presently under commercial development (Tehrani *et al.*, 2003). MRAM with enough memory capacity could eventually enable the advent of the instant boot-up computer. Today's laptops have semiconductor charge-based RAM that is volatile, losing its stored-up charge, and hence its stored information, when the power needed for its periodic refresh cycles is removed. MRAM is nonvolatile. Once one of its memory elements is magnetized, it retains its magnetization direction (and therefore its binary coding) without the need for additional power consumption.

Magnetic Logic. Another new spintronic device concept also potentially useful in computer technologies would be magnetic logic, based on spin transistor architectures, as in the proposals of Sugahara and Tanaka (2004) and Matsuno *et al.* (2004). The added value would be, for example, to create a magnetic central processor

unit (MCPU) that would have a soft architecture. It could be reconfigured to match the task at hand at any instant in time. It might sound far-fetched, but we are examining grand challenges, so we can think (and dream) outside the box. Today's high-performance computers utilize parallel processors. If each processor were also dynamically optimized, performance would be additionally enhanced. Why optimize only for graphics or for number crunching if you can achieve each goal when needed? Initial steps toward the exploration of magnetic quantum cellular automata at room temperature have been demonstrated by Cowburn and Welland (2000), and programmable logic gates using giant magnetoresistance devices are discussed by Hassoun *et al.* (1997).

Spin-Based Qubits. Since we are moving away from mainstream approaches, we can proceed to the next bubble of spin-based qubits. Here we are driven by the quest to utilize electronic or nuclear spin systems to implement quantum-computing paradigms and to transcend binary logic completely. This would, for example, permit certain classes of problems that are computationally off limits at present to become tractable. DiVincenzo and Loss (1999) discuss quantum computers and quantum coherence. Proposals that focus on spin chains and molecular magnets include the work of Leuenberger and Loss (1996) and Meier *et al.* (2003). Experimental systems of interest include single-molecule magnets that exhibit quantum tunneling of the magnetization, such as is highlighted in the work of Wernsdorfer *et al.* (2002).

Hierarchically Assembled Media. Next, we must find new ways to hierarchically assemble systems, such as magnetic recording media. Good ideas about new phenomena are important to develop, but we have to be able to implement them as well. In the quest to address society's issues (such as are associated with energy, transportation, stimulating the economy, enabling new approaches to healthcare, homeland security, defense, etc.), we must create new pathways to solutions such that they can be manufactured cost effectively. This means that we need to embrace the goal of creating entire hierarchical subsystems and systems instead of merely assembling individual materials and components. We can ponder that ultimately the goal could be, for example, to pull a fully assembled computer out of a test tube.

Nanobiomagnetic Sensors. As we consider the level of self-organization needed to achieve such a lofty, futuristic goal as just proposed, we look to the world of biology and biomimetic approaches to assembly. The intersection of biology and nanomagnetism has an immediate goal of giving rise to new concepts in sensing, such as are needed for homeland security and medical applications. A recent example can be found in the work of Hoffmann *et al.* (2005). Applications of magnetic nanoparticles to biomedicine have been reviewed by Pankhurst *et al.* (2003). This has taken us full circle, emphasizing a bridging of disciplines, and motivated by a quest to serve strategic national needs and goals. Now we highlight some examples limited as they might be. The examples will illustrate approaches to create, explore, and understand nanomagnetic systems.

C. Fabrication approaches

Nanoscience offers three major means to create new nanomagnetic materials, as reviewed by Martín *et al.* (2003). These are (i) top-down, (ii) bottom-up, and (iii) virtual fab. Top-down has been the traditional approach to miniaturization by sculpting via lithographic tools. But lithography needs enhancements to get to smaller length scales and to do so cost effectively. This is where the bottom-up approach enters centerstage. Bottom-up is self-assembly from molecular-precursor building blocks, as described by Whitesides and Grzybowski (2002). As such it encompasses the domains of chemistry and biology. However, self-assembly is not limited to these domains or length scales, because as we know on a majestic length scale, the entire Universe has self-organized into granular patterns of galaxies. Finally, we consider a third approach: virtual fab. This is the path taken by theorists and computationalists who create their new materials and properties in a computer simulation or analytically. For example, the virtual approach offers the best control of feature definition because the system is precisely specified at the outset. But the main advantage of virtual fab is to have the ability to obtain a fundamental understanding and to elucidate guiding principles. One can frame this, for example, as a quest to understand the rules that govern self-assembly. We know that the answer encompasses both thermodynamics and kinetics, and, hence, electronic structure. The main challenge is to seamlessly weave together almost every known computational tool and approach that addresses multiple time and length scales into an as yet unrealized hierarchical computation package.

II. SPECIFIC EXAMPLES

A. Spin injection

This example concerns the all-metallic lateral spin valve. Although magnetic semiconductors have many virtues, all-metallic spin-transport systems offer their own opportunity to explore elementary spin-transport concepts of injection, diffusion, and detection.

Figure 3 illustrates the example under consideration. Metallic spin injection in a lateral spin-valve prototype structure was first explored in the pioneering work of Johnson and Silsbee (1985), and more recently by groups in Groningen (Jedema *et al.*, 2001, 2002), Japan (Kimura *et al.*, 2004), and the United States (Valenzuela and Tinkham, 2004). Figure 3 is taken from Ji *et al.* (2004). It shows a spin valve having two ferromagnetic electrodes separated by a nonferromagnetic metallic spacer. The magnetic electrodes are patterned via electron-beam lithography from Permalloy (a Ni-Fe alloy), while the spacer is a 200-nm-wide gold stripe. Attached to these three elements in a rather nontraditional manner are current and voltage leads. In a traditional electronic cir-

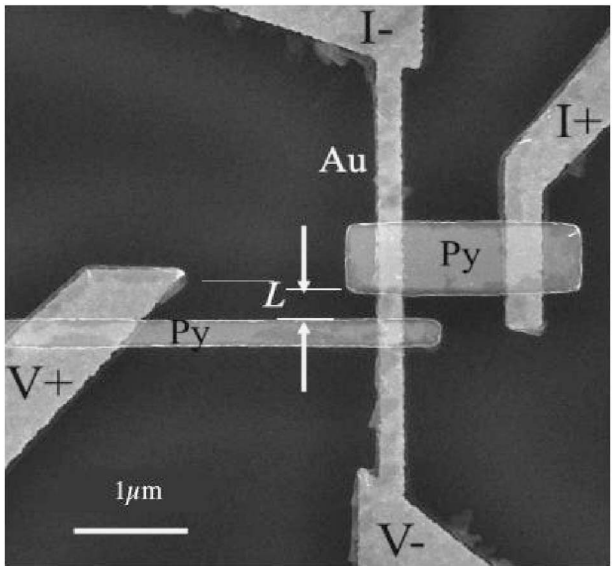

FIG. 3. Spin injection, diffusion, and detection in an all-metallic lateral spin-valve structure, from Ji *et al.* (2004). The two ferromagnetic Permalloy (Py) electrodes are fabricated with different aspect ratios to provide different coercive fields. This permits the applied magnetic field sweep to create magnetic orientations of two electrodes that are parallel at the maximum field and antiparallel in an intermediate field range. The two electrodes are separated by a length L and sandwich a Au stripe. Note the nontraditional placement of the current (I) and voltage (V) leads. Spins are injected from the top electrode, diffuse through Au, and are detected as a voltage across the bottom electrode that senses the nonequilibrium spin splitting of the chemical potential of Au.

cuit configured as shown, there would be no voltage detected; however, because the top Py electrode injects spins into the otherwise nonmagnetic gold, the chemical potential of the gold becomes spin-split, and the bottom Py electrode serves as a detector to sense the splitting. The current is ac modulated and the voltage is detected by means of a lock-in amplifier. The two Py electrodes are of different widths and therefore have different coercive (or switching) fields.

Figure 4 shows a field sweep with the vertical axis displaying the spin signal divided by the current, which yields units of electrical resistance. However, the quantity of interest is a spin resistance R_s rather than a traditional electrical resistance. The plot shows the spin-transport effect between two electrodes having parallel versus antiparallel magnetization orientation. There is an ~30% change in spin resistance ΔR_s shown in the plot. Interestingly, the antiparallel state is the low-resistance state, in contrast to what is commonly observed in giant magnetoresistance (GMR) spin valves. In the GMR case, the spin-dependent scattering at the interfaces governs the transport properties. For parallel alignment, one spin subband shunts the current, and hence a low-resistance state results [although there are intriguing exceptions that have been engineered by Al-HajDarwish *et al.* (2004)]. In the present case, parallel alignment adds a positive shift to the chemical potential

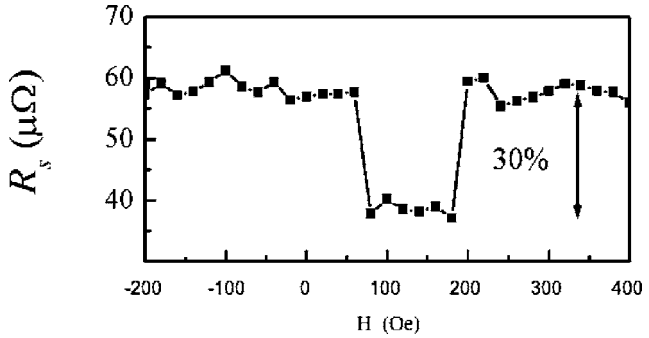

FIG. 4. The spin resistance of the lateral spin-valve structure shown in Fig. 3 plotted as a function of the external magnetic field that is applied along the long axis of the Py electrodes. The experiment by Ji *et al.* (2004) is performed at 10 K. An ~30% change in spin resistance (ΔR_s) is found in comparing parallel vs antiparallel orientations of the magnetization of the two Py electrodes. The antiparallel configuration gives rise to the low-resistance state, unlike in traditional giant magnetoresistance structures.

of gold relative to the Fermi energy of the detector, while antiparallel alignment yields a negative shift. Hence, the parallel orientation has a higher spin resistance.

Figure 5 shows ΔR_s as the spacing L between electrodes is systematically varied. Using an elementary expression for spin diffusion, as first invoked by Johnson and Silsbee (1985), the data yield a 63 ± 15 nm spin-diffusion length in Au at 10 K. This is rather short, and the spin-orbit interaction of Au, a high-Z or heavy element, is believed to be responsible.

This suggests a reason why *organic* spintronics is starting to be explored. If the spacer were low Z, like carbon-based nanotubes or organic π-bonded structures, a longer and therefore more versatile device could be created, as suggested in the paper by Xiong *et al.* (2004). The additional length available between two electrodes

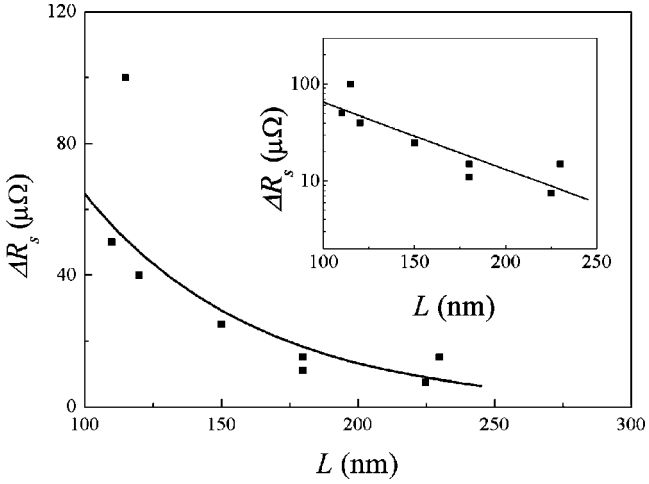

FIG. 5. The change in spin resistance ΔR_s of lateral spin valves, from data by Ji *et al.* (2004), summarized in linear and semilogarithmic (inset) plots in order to extract the spin diffusion length in Au at 10 K of 63 ± 15 nm.

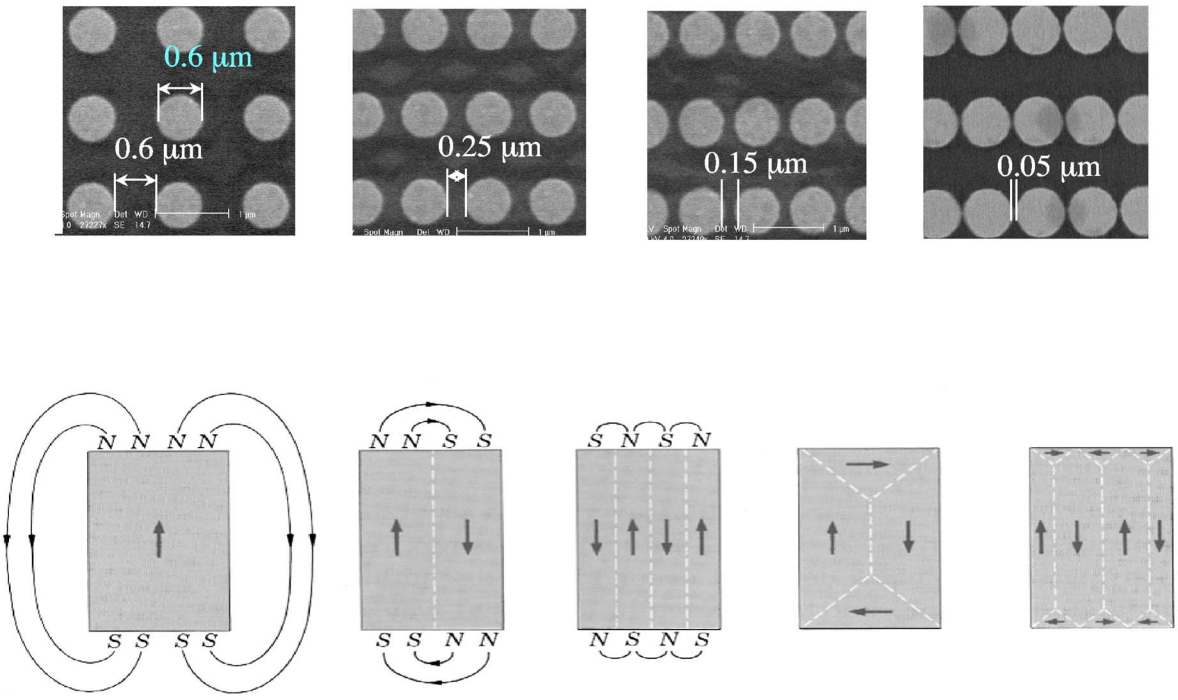

FIG. 6. (Color online) Arrays of Permalloy dots (thickness=60 nm) with systematically varying interdot separation in the top panel, based on Novosad *et al.* (2002). The dots form magnetic vortex structures in the absence of an applied magnetic field, as shown in Fig. 1(b). Such structures are used to explore the magnetostatic coupling of the dots. In the bottom panel schematics of a variety of magnetic domain structures for a rectangular ferromagnetic object, taken from the renowned textbook by Kittel (1996). The magnetostatic energy is most effectively reduced for closure domain cases shown as the last two examples to the right in the bottom panel. For the Permalloy dot geometry in the top panel, a magnetic vortex state is the corresponding equivalent to the closure domain.

could permit a third magnetic element to be positioned within them, leading to a triode or transistor configuration [Johnson (1996); Bauer *et al.* (2003)].

So, why was Au used as the spacer? The answer is simply because Au is relatively easy to fabricate as a prototype system. Au does not lend itself to oxidation, which could lead to degraded or uncontrolled junctions, as can be the case, for example, with low-Z aluminum.

The most remarkable feature of the lateral spin-valve structure of Fig. 3 is that the charge- and spin-current flows are separated. This can be viewed as an example of emergent behavior, in the sense that ordinary elemental and alloy metals, when put into proximity in a confined geometry, can exhibit entirely new physical phenomena.

What might be the practical consequences of such new magnetic electronics? We can imagine that if information could be transmitted and processed via spin currents, rather than charge currents, there would be less heat dissipated. We know that for today's electronics, heat management is an important issue. Stated more dramatically, one can hardly rest a laptop on one's lap because of the heat generated. A related development is the study of the spin-transfer effect, which provides a method to switch the magnetization direction of nanoscale magnets with spin currents. This phenomenon was first proposed by Berger (1996) and Slonczewski (1996) and and is actively being pursued experimentally, for example, by Katine *et al.* (2000).

B. Magnetic vortices

The next example will also be based on lithographic, top-down, assembly with Py elements. Figure 6 shows a configuration of submicron dot arrays, from the work of Novosad *et al.* (2002). In Fig. 6, the dot separation is systematically decreased in going from the left to the right top panel. These arrays give rise to unusual hysteresis loops, one of which is simulated in Fig. 7, based on the work of Guslienko *et al.* (2001). The loops have hysteretic side lobes but are nonhysteretic as the field crosses zero.

In this case, the understanding of such behavior utilizes the concept of the magnetic vortex. To get a feel for the physics we defer to a figure, shown in the lower panel of Fig. 6, from the classic text by Kittel (1996). It shows that magnetic objects lower their magnetostatic energy by forming domain structures, and that closure domains, as shown in the two examples to the right, are especially favorable. A closure domain is characterized by a closed flux circuit having no magnetic flux leakage outside the material. In a dot structure, such as in Fig. 6, the closure domain is the magnetic vortex structure, as depicted in Fig. 1(b) or Fig. 7(c). The vortex has a continuous variation of the magnetization direction in the plane of the dot, but the magnetization of its core is perpendicular to the plane.

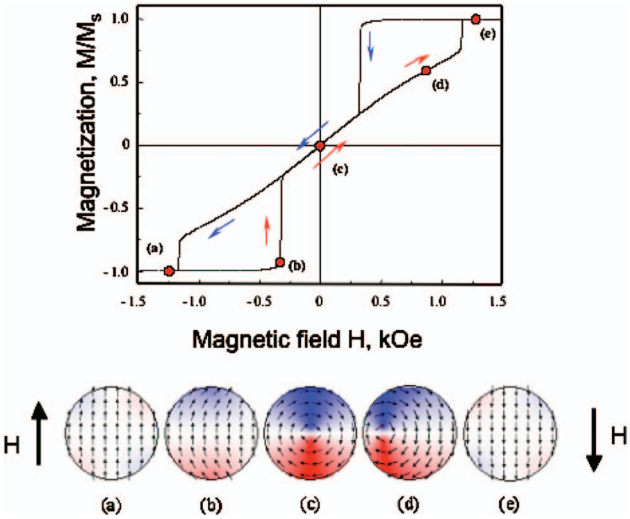

FIG. 7. (Color) Virtual fab representation of the magnetic hysteresis loop of a submicron dot array, such as is shown in Fig. 6, based on Guslienko *et al.* (2001). Micromagnetic simulations are used to represent the spin configurations of the Permalloy dot array along the path of a hysteresis loop. (a) Spin configuration aligned with the applied field direction; (b) at the point of nucleation of the vortex core at the right edge of the dot; (c) the symmetric vortex in zero field; (d) the vortex core, as it shifts to the left with increasing applied field, but before being annihilated at the left edge of the dot; and (e) the reverse of (a). Note that the central portion of the loop is nonhysteretic, as the vortex core shifts to the left or right, while the side lobes are hysteretic as the core nucleates or is annihilated. Magnetostatic interactions will affect the magnitude of the nucleation and annihilation fields.

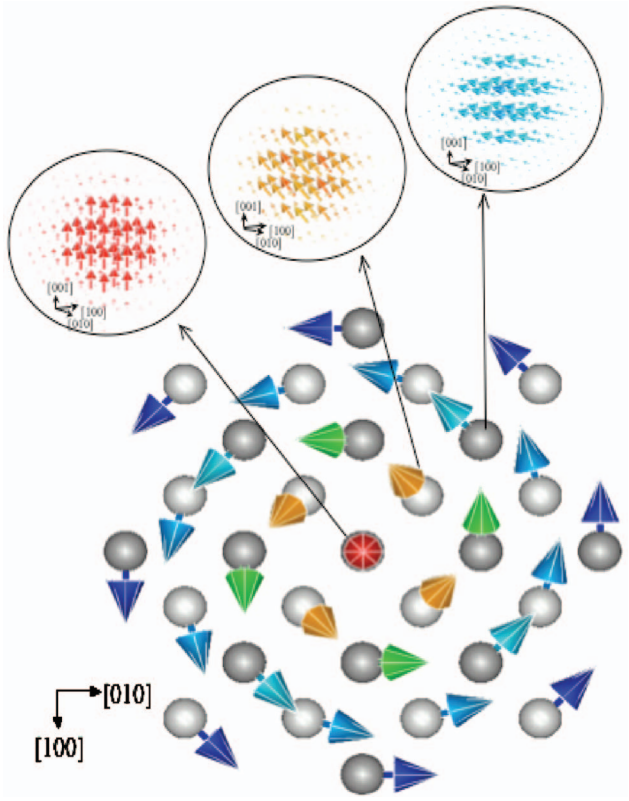

FIG. 8. (Color) Virtual fab representation of the geometry, spin arrangement, and spin densities (insets) of 29 Fe atoms, from electronic structural calculations of Nakamura *et al.* (2003) carried out via the local-density approximation. The outer shells of Fe atoms have their spin structures constrained to form a magnetic vortex, while the spins of the inner Fe atoms are self-consistently calculated to relax into the vortex structure indicated, with the spin of the central Fe atom forming the out-of-plane singularity, and the spins on the next shell of Fe atoms forming a canted structure.

Now we can visualize the magnetization process with the help of the micromagnetic simulations depicted in the lower part of Fig. 7. The nonhysteretic part of the magnetization loop is associated with the vortex core shifting to the left [Fig. 7(d)] or right, depending on the direction of the external magnetic field applied in plane (down or up, respectively, as shown). The hysteretic side lobes are associated with vortex creation or annihilation at the edge of the dot.

We can take Fig. 7 as an example of virtual fab. This is because the structure is created and modeled computationally. Insights are derived by comparing the simulations to experiment. When the virtual material behaves very much like the actual material, the underlying governing mechanisms can be identified.

Vortex states are of interest because they are prevalent both in Nature and in artificially made structures. Moving beyond solid-state physics examples, such as the landmark work of Abrikosov (1957) on the flux lattice in type-II superconductors, we find vortices in astrophysics, in the swarming of birds and fish in nature, and in the gentle swirls of the gravel in a Zen garden. The magnetic vortex is an inhomogeneous magnetization state with a singularity, and has two key properties: chirality c and polarity p. The chirality can be $c=\pm 1$ (clockwise or counterclockwise) and the polarity can be $p=\pm 1$ (positive or negative). These two parameters (together with the topological charge of the core) underlie the dynamic response of submicron structures to rapid magnetic field pulses. An interesting case is of two vortices in a GMR-type trilayer geometry with ferromagnetic vortices labeled 1 and 2, where the products $c_1c_2=\pm 1$ and $p_1p_2=\pm 1$ give rise to different energetics and dynamics, as has recently been explored by Guslienko *et al.* (2005). Extensive analyses of magnetic microstructures are covered in Hubert and Schäfer (1998). The book by Aharoni (1996) also provides a wealth of information on the subject. Recent Kerr microscopy studies of spin dynamics in single-layer Py elements appear in the work of Park *et al.* (2003) and Buess *et al.* (2004).

Another example of virtual fab simulation is shown in the work of Nakamura *et al.* (2003) in Fig. 8. Twenty-nine Fe atoms are arranged within a LDA (local-density approximation) calculation as shown. The outer circle of Fe atoms has their magnetization direction fixed to form a vortex arrangement, while the magnetization direction of the inner shells is able to self-consistently lower their energy. The result is that the illustrated vortex structure is created. The vortex is complete with the central atom

having a perpendicular magnetization direction and the next shell of atoms forming a magnetic structure that is canted out of plane.

This is a different class of virtual fab than shown in the previous example of a micromagnetic simulation. The structure shown in Fig. 8 is not an equilibrium configuration found in nature. The energetics of stability of noncollinear magnetization structures requires a larger-sized object than a mere 29 atoms. The magnetostatic energy savings must more than balance the increase in energy needed to create a domain wall or canted magnetization configuration. That is the constraint for small-sized objects that would prefer, instead, to adopt a single-domain state. Thus, the vortex state has a lower size limit of stability. And, of course, if size were to become too large, then multidomain structures could result. A recent example of calculated magnetic phase diagrams as a function of feature size can be found in the work of Ding *et al.* (2005).

Despite this, the beauty of the virtual material depicted in Fig. 8 is that its properties are tractable by first-principles calculations. The spin densities are shown in the elliptical insets at the top of the figure. Most interestingly, the spin-orbit coupling and, hence, the orbital magnetic moment of each color-coded region can be predicted numerically (Nakamura *et al.*, 2003). The general insights gained should apply to real vortex systems. Thus, techniques can be brought to bear on the problem to explore orbital moments, i.e., using synchrotron-based spectroscopy, as described by Kortright *et al.* (1999), and neutron-scattering strategies, as described by Fitzsimmons *et al.* (2004). Such future experimental tests could be used to determine whether the predictions capture the actual physics of the system.

Figure 9 illustrates the use of x-ray magnetic circular dichroism (MCD) to image the magnetic domain structure. For a magnetized material, the absorption of left and right circularly polarized light is asymmetric. Using tunable x rays at a synchrotron source (the Advanced Light Source at Berkeley, in this case), one can monitor the resonant signal upon traversing core edges, and hence obtain element-sensitive information. The examples in Fig. 9, from the work of Buchanan *et al.* (2005), show that size and shape are important in determining the domain structure. Examples labeled (a) have single-domain structures of opposite magnetization orientation, hence the MCD contrast is either light or dark. Examples (b) are of magnetic vortices of opposite chirality ($c=\pm 1$). Example (c) shows an ellipse with a double vortex structure, as is modeled in the lower part of Fig. 9, and example (d) is of an ellipse with a 180°-domain structure.

In order to pinpoint the magnetization structures in Fig. 9, one must go beyond merely examining the images shown. For example, rotating the structures within the spectrometer might be necessary in order to see whether the contrast patterns observed are invariant or not. A vortex structure would give rise to an invariant pattern, while, for example, the contrast pattern from a 180°-domain structure would follow the mechanical rotation.

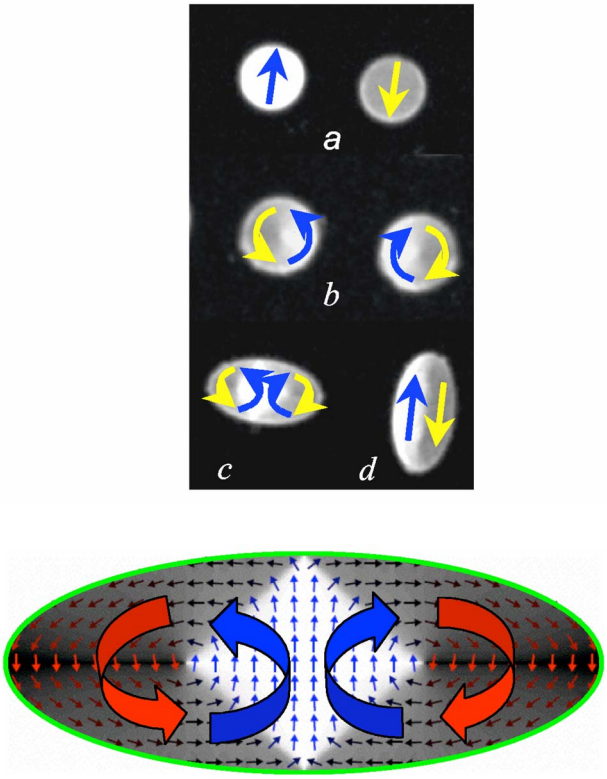

FIG. 9. (Color online) A composite of magnetic images of lithographically patterned Permalloy structures is shown that exhibits size-dependent, metastable remanent states, taken from the work of Buchanan *et al.* (2005). The images are obtained utilizing the magnetic contrast from resonant x-ray magnetic circular dichroism (XMCD) experiments that utilize photoemission electron microscopy (PEEM) at the Advanced Light Source at Lawrence Berkeley National Laboratory. The samples are subjected to rapidly pulsed magnetic fields and are then imaged in zero field. (a) Two images of single domain states of opposite orientation (with light and dark magnetic contrast, respectively), and (b) two images whose magnetic contrast is indicative of magnetic vortex states of opposite chirality, as indicated by the arrows. The corresponding vortex simulation is shown in Fig. 1(b). (c) The dark-light-dark contrast indicative of a double-vortex spin configuration, as indicated by the arrows and the micromagnetic simulation in the bottom panel, and (d) two opposing magnetic domains that run along the major axis of an elliptically shaped structure. The bottom panel provides a micromagnetic simulation of a double-vortex spin configuration to compare to the image in (c).

Other great strengths of the MCD approach are that (i) the orbital moment can be accessed as mentioned above, (ii) the spatial resolution for soft x rays can be brought into the nanoscale range, and (iii) the temporal resolution can be linked to the electron bunch spacing within the storage ring used to produce the x rays. To enhance the spatial resolution, the experiments utilized photoelectron emission microscopy (PEEM) to detect the contrast variation, as described by Anders *et al.* (1999). The resolution used is ~100 nm, but in the next-

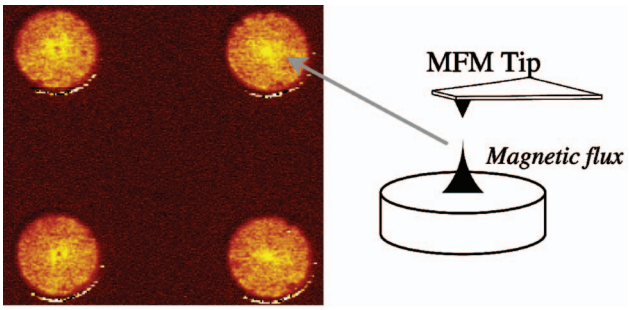

FIG. 10. (Color) Magnetic force microscopy (MFM) images of Permalloy submicron dots, from Novosad *et al.* (2003), that indicate a hint of the magnetic vortex core singularity via the contrast change at the dot centers. Also shown is a schematic of the sample and the MFM tip that senses the out-of-plane magnetic flux gradient.

generation PEEM instrument at the Advanced Light Source this should approach a few nanometers. The temporal resolution, not really exploited in the example provided, is limited by the speed with which a magnetic field pulse can be delivered to the sample. The experiment is configured with lithographic strip lines and a laser-activated photoconductive switch that enables the production of ~100 ps duration field pulses. The spatial and temporal resolution is well suited to monitoring the dynamics of future-generation, patterned magnetic data storage media. Thus, great interest exists in the future of such experiments. Stöhr (1999) has provided an excellent overview of the opportunities.

The level of sophistication attained by modern instrumentation at major research facilities is somewhat awe inspiring. Bench-top science can be put to good use as well, as is illustrated in Fig. 10, in which magnetic force microscopy (MFM) is used to image the gradient of the perpendicular component of the magnetization of dot structures, based on the work of Novosad *et al.* (2001). The light central portion hints at the existence of a vortex core. Pioneering work in this area (with striking results) has been reported by Okuno *et al.* (2002). A variety of submicron-array structures have been examined via MFM, such as in the work of Novosad *et al.* (2003). A general discussion of the theory of scanning probe microscopies is provided by Hofer *et al.* (2003), and the promising technique of spin-polarized scanning electron microscopy has been reviewed by Bode (2003).

Another bench-top approach and a visible wavelength analog to the x-ray–based MCD (XMCD) is the magneto-optic Kerr effect (MOKE). MOKE utilizes linearly polarized light, and has been used to study ultrathin magnetic films, as described by Qiu and Bader (2000). The contrast is produced by switching either the polarization direction of the light or the applied magnetic field direction. In the DMOKE approach, the wavelength of the laser light is comparable to the dot spacing of the lithographic array, hence the light not only reflects but also diffracts. DMOKE can examine the collective properties of the array and has been used to determine, for example, that the chirality can be coherent across dot arrays whose elements are spaced far enough apart that they should be noninteracting, as discussed by Grimsditch *et al.* (2002). Also, elliptically shaped array geometries have been examined by Vavassori *et al.* (2004).

C. Bottom-up strategies

The above examples are based on lithographic patterning. Now we will move to self-assembly and hybrid strategies to create new and interesting materials. The examples, of course, refer to nanomagnetic systems, but the strategies and principles are general to all of nanoscience.

What are the principles of nanoscience? There are three: geometric confinement, physical proximity, and chemical self-organization. Confinement permits the formation of new materials via manipulation of dimensionality. Proximity permits the formation of new materials via the creation of composites that couple together and behave as a single new entity. Chemical self-organization permits the formation of new materials via harnessing the ability of nature to build from the molecular level on up.

1. Use of spring magnets

The first example of exchange-spring coupled magnets is of interest because of its energy implications in the quest for ultrastrong permanent magnets—one of the grand challenges introduced earlier. What is a spring magnet? The concept was articulated in theoretical terms by Kneller and Hawig (1991) and Skomski and Coey (1993). Interestingly, the first experimental realization of the exchange-spring principle, by Coehoorn *et al.* (1989), preceded the theoretical work.

Figure 11 shows schematically two magnetic hysteresis loops: one is wide but short and the other is tall but narrow. The engineering figure of merit of a permanent magnet, used to determine its strength, is known as the maximum energy product $(BH)_{\max}$ taken in the second quadrant in the loop (upper left quadrant). A strong permanent magnet will have a square loop that is both tall and wide. In general, obtaining one characteristic (tall or wide) rather than both (tall and wide) is easier in a single material.

The world's strongest commercial permanent magnet presently is $Nd_2Fe_{14}B$, first reported by Croat *et al.* (1984) and Sagawa *et al.* (1984). The advent of NdFeB provided the basis for dramatic miniaturization of, e.g., motors and audio speaker systems, and serves as the basis for modern permanent magnet undulators and wigglers at third-generation synchrotron sources, such as the Advanced Light Source at Berkeley, mentioned earlier, or the Advanced Photon Source at Argonne.

NdFeB has a wide hysteresis loop, indicating a strong coercive force to resist a field applied opposite to its magnetization direction. But NdFeB does not have a particularly tall loop, indicating that its magnetization per unit volume is not exceptional, say compared to or-

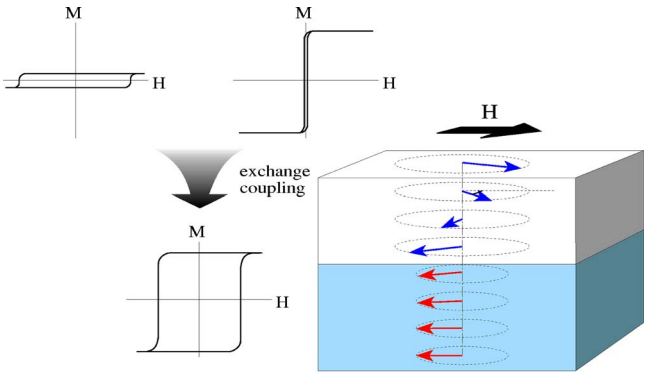

FIG. 11. (Color online) The exchange-spring principle is illustrated. A magnetically hard ferromagnet possessing a wide hysteresis loop, as shown to the left, exchange couples to a magnetically soft ferromagnet possessing a tall hysteresis loop, as shown to the right, forming a composite ferromagnet that has both a wide and tall hysteresis loop, as indicated below. The coupling principle can be used to create ultrastrong magnets that theoretically can outperform the strongest present-day commercial permanent magnets. The image to the right illustrates a bilayer structure that has similarly magnetically hard (bottom layer) and soft (top layer) layers. If the soft layer thickness exceeds a magnetic domain-wall thickness, a twisted magnetization structure can form in the soft layer, as shown, in response to an applied magnetic field, indicated by H, that is opposed to the magnetization of the composite. This illustrates why spring magnets are nanocomposites in nature, because the domain-wall thickness is of nanoscale dimensions. The twist must be suppressed in order to achieve an ultrastrong permanent magnet configuration.

dinary iron, depicted very schematically in the right loop in Fig. 11. Why is this the case? While NdFeB has a complex crystal structure, as summarized by Herbst (1991), with three formula units of $Nd_2Fe_{14}B$ per unit cell we can make a few qualitative observations. The coercivity is attributed in large part to the presence of Nd because its unquenched orbital angular momentum leads to an enhanced magnetocrystalline anisotropy. But the total magnetic moment of Nd is fairly comparable to that of Fe, while the atomic radius of the atom is about three times as large. Also, note that B has no magnetic moment. This hints as to why the magnetization per unit volume of NdFeB is not impressive compared to that of Fe, while the width of the hysteresis loop is.

Thus, the idea is to create a composite of a magnetically hard ferromagnet (such as NdFeB) and a magnetically soft ferromagnet with a high magnetization (such as Fe or Co). If two components magnetically couple together, the resultant composite can have both a wide and tall loop, meaning that the composite magnetic structure will be ultrastrong. The magnetically soft component becomes a slave to the hard component and follows its magnetization direction. (This illustrates the importance of physical proximity, which was alluded to above.)

But why do the two components have to be confined on the nanoscale? The reason is that if the soft phase is unconfined, it can form noncollinear or twisted magnetization structures to try to follow either an external or demagnetization field. This is shown schematically for a hard-soft bilayer in Fig. 11, where the magnetically hard layer is on the bottom and its magnetization orientation is depicted by arrows. An external field H applied in the opposite direction causes the magnetization of the soft layer to twist away from its original direction. The magnetization of the soft layer is pinned at the interface with the hard layer, but it fans over to the direction of H, as reviewed by Fullerton *et al.* (1999) and Jiang *et al.* (2002). However, if the physical dimension of the soft layer is small enough, it will be energetically unable to support a twisted magnetization configuration.

The critical dimension to sustain a twist can be calculated; physically it represents the width of a magnetic domain wall of the hard phase. The domain-wall width is of the order of a few nanometers. (This is why spring magnets are a product of nanotechnology.) Of course the hard component can be larger than nanoscale, but the energy product will be larger if the volume fraction of the hard material is limited. This has practical benefits as well because the hard material is usually more costly and can present corrosion problems if rare earths are involved. Thus, minimizing the amount of the expensive component and coating the rare-earth phase with a barrier material to prevent or arrest corrosion has engineering benefits.

We see illustrated in this example the benefits of confinement and proximity, but how does chemical self-organization enter the picture? Again, self-assembly is involved to overcome practical engineering considerations of how one might manufacture such nanocomposite magnets. Size control on the nanoscale always presents serious challenges. If we wanted to construct such a nanocomposite magnet but a small region had a soft-phase inclusion that exceeded a domain-wall thickness, it could create a hot spot that would nucleate a reverse domain. This could lead to an avalanche that would switch the entire material. Self-assembly, with its precise ability to control size and size distribution at the necessary level, however, can make the difference here between success and failure in the creation of a novel and potentially useful new class of nanocomposite materials.

The question becomes: How would the self-assembly be implemented? Surfactant-mediated colloidal nanoparticle production looks promising. [It involves the high-temperature thermal decomposition of organic precursors, and has been successfully applied to produce a range of semiconductor materials with interesting properties, such as CdSe quantum dot superlattices by Murray *et al.* (1995) and related semiconductor quantum dots by Alivisatos (1996).] The same approach has been applied to magnetic nanoparticle synthesis. For example, soft magnets, such as Co (Puntes *et al.*, 2001), and hard magnets, such as FePt (Sun *et al.*, 2000), have been prepared by means of similar chemistry.

The top of Fig. 12 shows an example of a regular 2D array of Co nanoparticles synthesized in this manner, as imaged by means of transmission electron microscopy (TEM), from the work of Samia *et al.* (2005). Interest-

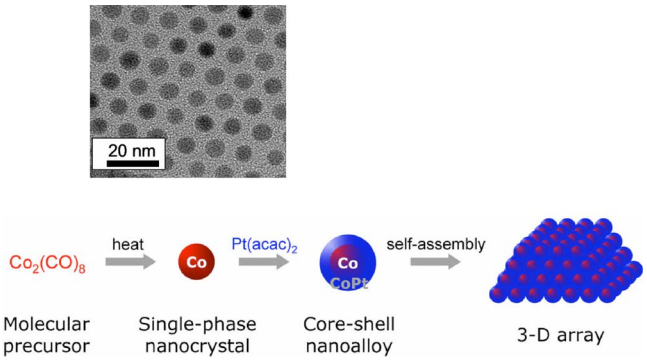

FIG. 12. (Color online) Schematic surfactant-mediated chemical processing steps are shown to create core-shell nanocomposite spring magnets that then self-assemble or agglomerate into bulk structures. The TEM image at the top is of a film of self-assembled, monodispersed 9.5-nm Co nanocrystals made via surfactant-mediated processing, as reported by Samia *et al.* (2005).

ingly, due to ligand stabilization effects the Co particles form in an ε phase, which is a distorted face-centered-cubic structure not present in the bulk phase diagram, as discussed in the references found in their work.

In the area of hard magnets, the less reactive Pt-containing magnets are actively being pursued more so than the rare-earth containing materials, where oxidation is a concern. The magnetic recording industry is presently focused on perfecting the properties of high-anisotropy FePt alloys, as in Weller *et al.* (2000). Thus, the motivation to develop such materials and processes is strong. Progress in the direct synthesis of the desired face-centered tetragonal $L1_0$ phase of PtFe nanoparticles has been reported, for example, by Jeyadevan *et al.* (2003), Teng and Yang (2003), and Sasaki *et al.* (2005).

Exchange coupled nanocomposite films made by mixing magnetically hard and soft nanocrystals was reported by Zeng *et al.* (2002). Their work shows great potential for using these colloidal nanocrystals as permanent magnets with high energy-product values. However, mixing different types of colloids can induce inhomogeneity that results in undesirable magnetic switching properties. A more controlled strategy is to engineer core-shell particles made of hard and soft magnetic materials. The magnetic properties can then be directly tuned on the level of a single particle. Such a strategy is shown schematically in Fig. 12 where a magnetically soft Co core is coated with a magnetically hard CoPt composition. By containing the soft phase in a core-shell geometry, hot spots can be avoided that might otherwise form due to particle agglomeration. Besides using CoPt as the hard phase, NdFeB or SmCo would also be suitable. The magnetic hardening mechanism of CoPt (or FePt) is associated with the induced magnetic moment on nearly magnetic Pt in proximity to Co (or Fe). (Pt and Pd are sometimes referred to as *incipient ferromagnets* due to their enhanced magnetic susceptibilities.) Then the strong spin-orbit coupling due to the high Z of Pt yields a large magnetocrystalline anisotropy and hence can yield a sizable coercivity. The theory of induced Pt moments in FePt was recently discussed by Mryasov *et al.* (2005).

Efforts to create surfactant-mediated nanoparticles have been more successful to date for the chemically less reactive Pt-containing magnets than for rare-earth containing materials where oxidation is a concern. This very promising bottom-up chemical approach to self-assembly is subject to much research presently.

One last question before we move on from spring magnets: Why are they referred to as spring magnets? The reason is simply that in the case for which the soft phase has large enough dimensions that it can support a twisted structure in the field, the twist will spring back to the original state of full remanence if the field is removed. Most other ferromagnets will trace out subloops with reduced remanent magnetization in zero field when subjected to such a partial field cycling. Rather than a mechanical spring, we have an exchange spring due to the interfacial magnetic coupling of the hard and soft phases. The interfacial pinning is reminiscent and in some cases formally similar to that encountered in the very popular exchange-bias problem that involves the magnetic pinning of a ferromagnet to an antiferromagnet. Exchange bias has been reviewed by Berkowitz and Takano (1999) and Nogués and Schuller (1999). The relationship between exchange-spring and exchange-bias systems was highlighted by Jiang *et al.* (2001), especially as it relates to novel double superlattice exchange-bias systems that emerged subsequent to the two reviews just cited.

2. Hierarchical assembly

Now we explore a hybrid top-down/bottom-up concept to organize surfactant-mediated nanoparticles, such as the FePt system just discussed in the prior example. The motivation is to treat each particle as a magnetic bit for futuristic Tbit/in.^{2} patterned storage media applications. How can the bits be organized along the radial tracks of a magnetic recording disk? In this example, soft organic matter will be used as a template to achieve the goal. The soft template is formed by diblock copolymer self-assembly into a nanostructured stripe domain film. The stripes, driven by segregation, are alternately hydrophilic and hydrophobic. Diblocks commonly segregate into a variety of ordered structures, based on the chemistry and temperature and molar fraction between constituent components, as described by Bates and Fredrickson (1999). But the ordering tends to be short ranged, and only an overall texturing is noted over larger distances.

For a hard-disk template, however, long-range order is essential. Long-range order can be accomplished by utilizing lithographic patterning of the substrate to form grooves along which the diblocks organize themselves. Such an approach is described by Cheng *et al.* (2003), using the diblocks as a selective resist to ion-beam etch bits from a coated magnetic film, and by Naito *et al.*

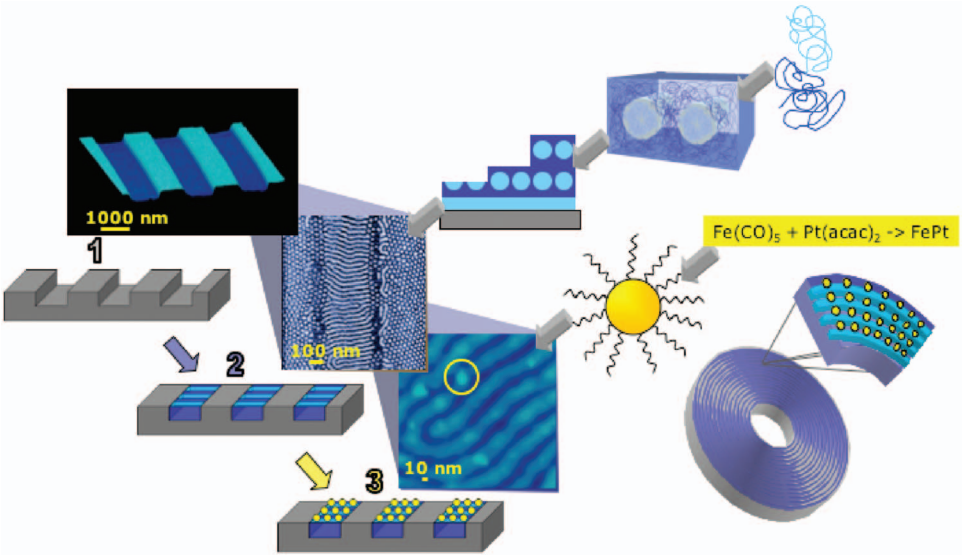

FIG. 13. (Color) A schematic of a potential three-step hierarchical assembly process is indicated for organizing magnetic nanoparticles, with AFM insets shown for each step, based on the work of Darling *et al.* (2005). The first step is to form lithographic grooves in a substrate, which serve to assist the long-range ordering of diblock copolymers that self-assemble into stripe domains in the second step. In the third step, surfactant-mediated magnetic nanoparticles are attached selectively from solution to the hydrophobic stripes because of the chemical affinity to the organic surfactant. The breakdown of the second and third steps at the right represents the chemistries involved, while the image at the bottom right is a cartoon of a magnetic hard disk for data storage that is fabricated based on the three-step process. The image is suggestive of the role chemistry and self-assembly might play in the future quest for affordable patterned storage media with densities in the Tbit/in.^{2} range. The example is a hybrid strategy that would involve lithographically assisted self-assembly, with imprint lithography, polymer spin-coating, and dip-coating steps for ease of manufacture.

(2002), who bring an industrial perspective to the problem.

A three-step process is schematically presented in Fig. 13, based on the work of Darling *et al.* (2005). The polymer in the example is polystyrene-block-polymethyl methacrylate (PS-b-PMMA), where the PS is the hydrophobic end of the polymer string and the PMMA is the hydrophilic end. The first step is to pattern grooves in the substrate. Second, the diblock stripes must self-assemble with respect to the grooves. Third, one must attach the individual magnetic nanoparticle bits to the tracks thus formed. The organic surfactant coating of the magnetic nanoparticle has a natural chemical affinity for hydrophobic stripes and avoids hydrophilic stripes.

Figure 13 also shows schematic chemical steps associated with diblock and nanoparticle formations. The bottom right cartoon is the disk, which would be created by stamping lithographic grooves into a substrate, then spin coating the diblock layer in place, and finally dipping to attach the surfactant-coated magnetic nanoparticles.

The overall process might be inexpensive to implement. For example, the lithographic grooves would not require state-of-the-art processing because ultimate resolution is not required. The segregation of the diblock into nanoscale tracks within the grooves would achieve the fine tracks that could transcend the physical limits of lithography. This is because chemical molecular interactions control the polymeric assembly. Note that the polymer tracks can be controlled to run along the length of the grooves (as in the disk example) or perpendicular to the grooves, depending on processing conditions. The latter orientation is shown in the figure as an AFM image of a scanned polymer surface (see step 2). Also shown via an AFM image is the selective adsorption of magnetic nanoparticles onto only one of the polymer phases (see step 3).

Many difficult scientific problems must be overcome in order to realize any industrial-scale application, and this example is no exception. Some of the chemical processing issues are outlined by Darling and Bader (2005). While great progress is being made to master the art of lithographically guided self-assembly of diblock copolymers, such as in the work of Lin *et al.* (2005), much work still needs to be done to create magnetic nanoparticles such as FePt that would be suitable as magnetic bits.

The key point, whether or not such a hierarchical approach is ever adopted commercially, is that the modern field of nanomagnetism is diverse and is coupling to many other exciting fields, such as the chemistry and thermodynamics of soft-matter diblock copolymers. A community of researchers is working to explore the implementation of many novel polymeric templating schemes.

In discussing the challenges, the focus was on the templating of magnetic nanoparticles, but the chemistry of diblock copolymers is itself also a challenge. PS-b-PMMA films segregate into stripes that have both components present on the surface, while other diblock copolymers have homophilic surfaces because the second, rod-shaped phase is buried. This can be seen schemati-

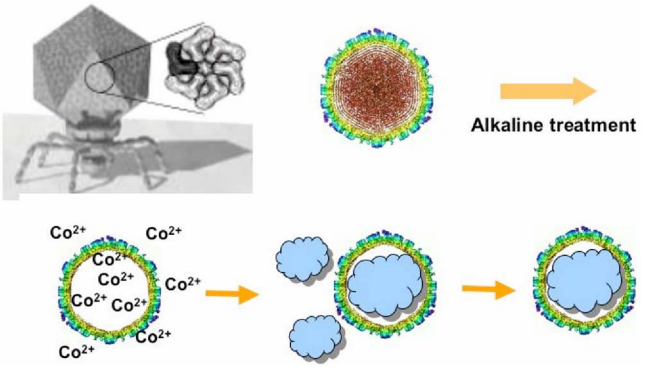

FIG. 14. (Color online) Schematics of the process to make artificial magnetic viruses. The rendition in the top left is of a virus showing its self-assembled protein capsid container and its attachment structure that is used to anchor it to a living cell, from Rosenberg *et al.* (1996). At the top right is a cryo TEM cross section of a capsid shell with DNA inside, from Cerritelli *et al.* (1997). At the bottom is a cartoon of biomineralization that results in Co nanoparticle growth inside the capsid shell that was hollowed out by an alkaline treatment process, based on Liu *et al.* (2005).

cally in the stage 2 composite in Fig. 13 where encased rodlike structures form that can be exposed either at the surface or not.

3. Use of magnetic viruses

The last example will push the envelope on organic soft matter templating. In this case, a naturally occurring virus will be manipulated to use its protein capsid shell as the container for the biomineralization of magnetic nanoparticles. Like the prior examples, the methodology is not limited to the creation of nanoparticles that are magnetic in nature. But these are the entities of interest in this study, so magnetism will serve as the focus.

Note also that while surfactant-coated nanoparticles, such as was discussed above, can be created with impressive size-distribution control, the average size tends to be limited to below ~15 nm. This is because as the particle itself gets too large, the energetics associated with the binding to the surfactant can no longer control the morphology. In the range from 10 to 100 nm, size control and uniformity present their own special challenges. Here is where viral templating enters.

But what is a virus? Figure 14 shows a schematic of a T7 bacteriophage virus from Rosenberg *et al.* (1996). It has a protein capsid shell that encloses coiled-up DNA, as shown in the cryo-TEM cross section in the top right, from the work of Cerritelli *et al.* (1997). [Baker *et al.* (1999) provide an impressive source of three-dimensional reconstructions of many viruses from cryo-electron micrographs.] The T7 capsid consists of hundreds of protein molecules assembled into a geometric container structure, as indicated in the figure. The virus also has an attachment structure to bind to the cell that is to be attacked.

In the following example we will be interested in T7, a virus that attacks bacteria, and whose capsid shell contains seven different types of proteins. In a series of wet chemical steps, Liu *et al.* (2005) subjected T7 to an alkaline solution that triggers a response similar to that which occurs if the virus attaches to a bacterium. The virus ejects its DNA into the solution and its attachment structure drops off, resulting in a hollow capsid shell. The shell can be reconditioned (renatured) and then washed and exposed to an aqueous environment rich in magnetic ions. A biomineralization process can be initiated chemically that leads to the precipitation of, for example, cobalt or iron oxide within the capsid shell. The growth of the resultant particle is limited to the container size. For T7, an ~40 nm magnetic particle can be created. This is outside the range of control of surfactant-mediated nanoparticle growth, as already mentioned. The beauty is that since all the templates are chemically identical, the size distribution should be small, as was found by Liu *et al.* (2005).

Such magnetic virus particles can serve as the basis for exotic sensing schemes. The reason is that the outside of the capsid shell presents itself for biochemically selective lock-and-key type attachments to specific affinity molecules. For example, the capsid exterior can be functionalized to attach to toxic molecules whose presence needs to be detected in homeland security scenarios. A canonical sensing example based on the avidin-biotin affinity was recently explored as a proof of principle by Chung *et al.* (2004).

Figure 15, from the work of Liu *et al.* (2005), shows TEM images of T7, the hollow resultant capsid that is known as the ghost virus (or ghost phage), and three examples of the final biomineralized composites that are loosely referred to as the magnetic virus, but that might more precisely be called the *chimeric magnetic phage*. A general overview of biomineralization and biomimetic materials chemistry is presented by Mann (1995). Also, recent overviews of the self-assembly of novel biomaterials appear in the work of Elemans *et al.* (2003) and Zhang (2003).

Mao *et al.* (2004), and others cited therein, have made dramatic advances in viral templating of nanoparticles. Also, single protein capsid templating of magnetic nanoparticles has been reported by Douglas and Young (1998) and Allen *et al.* (2002). In that approach, a *single* protein is self-assembled to form the hollow capsid that then serves as the template for the subsequent processing. This contrasts with the T7-based approach discussed above that uses a *native* capsid that consists of multiple protein types. The advantage of the native capsid is that it possesses greater protein structural diversity that can be harnessed in subsequent chemical and biorecognition applications.

We can compare the magnetic viruses discussed above to the naturally occurring protein ferritin. Although not a virus, ferritin has an ~7-nm magnetic core surrounded by a 2.5-nm-thick protein shell. The ferritin core is an antiferromagnetic iron oxyhydroxide composition with as many as 4500 Fe^{3+} ions. Uncompensated spins at the surface of the core, as described by Kilcoyne and Cywinski (1995) and Gilles *et al.* (2000), yield a net core mo-

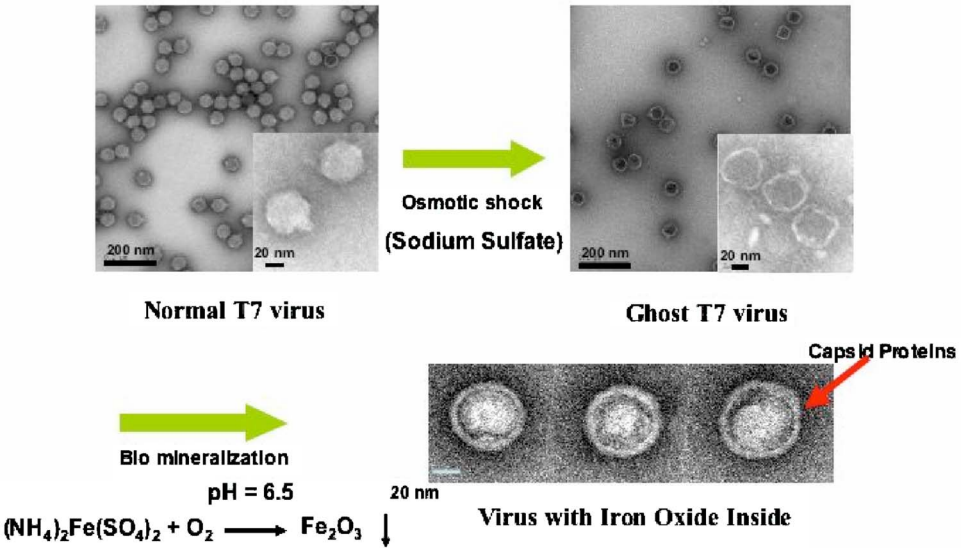

FIG. 15. (Color online) The fabrication of magnetic viruses is documented in TEM images, from Liu *et al.* (2005). The image at the left shows normal T7 bacteriophage and the image to the right shows the hollow capsid, or ghost virus, after alkaline treatment that triggers the ejection of the DNA and loss of the attachment structure. At the bottom shown are three magnetic viruses consisting of the native protein capsid filled with iron oxide after the biomineralization process.

ment of $300\mu_B$ in high fields. The small size of the core and the small magnetic moment make the system an ideal platform for the study of superparamagnetism. Magnetic relaxation studies of ferritin, as summarized by Luis *et al.* (1999), provide interesting evidence for quantum resonant tunneling between thermally excited spin states, as first reported by Gider *et al.* (1996). Thus, we conclude this subsection with the message that a rich variety of possibilities exist in the study of protein-coated magnetic nanoparticles of varying sizes. The outlook is very promising for this interdisciplinary endeavor that represents a marriage between magnetism and biology.

III. SUMMARY AND CONCLUSIONS

We have taken a journey through the topic of opportunities in nanomagnetism from the perspective of one of its practitioners. Thus, the scope is limited to topics of present activity within the author's research group and those of affiliates. The idea is not that these are the definitive activities that will distinguish the field in the future, but instead that the field is veritably bursting with activity and cross-disciplinary innovation. This is the sign of a healthy field that is blossoming. The parent field of magnetism has deep historical roots that go back really to antiquity (and at least to William Gilbert's 1600 work).

The presentation of this Colloquium has been organized to highlight grand challenges and difficult scientific problems for the future. The emphasis is on the use of nanomagnetism as a platform to illustrate some of the interest in the emerging field of nanoscience. The fabrication approaches of top-down, bottom-up, and virtual fab were illustrated, as well as a hybrid top-down/bottom-up example. The relations to advances in instrumentation were illustrated; these ranged from major facility synchrotron x-ray spectromicroscopy to scanning probes, magneto-optics, magnetotransport, magnetometry, and electron microscopies. The principles of nanoscience were enunciated (geometric confinement, physical proximity, and chemical self-organization) and illustrated with examples involving the quest for ultrastrong permanent magnets, ultra-high-density magnetic recording media, and novel nanobiomagnetic sensing strategies. The relations to chemistry, soft polymeric matter, and biological containment provided by viruses were illustrated. The interested reader is referred to the reference list for additional reading.

ACKNOWLEDGMENTS

The work was supported by the U.S. Department of Energy, Office of Basic Sciences, under Contract No. W-31-109-ENG-38. The author is indebted to his many colleagues who are cited as coauthors in the reference list. Special thanks go to Kristen Buchanan, Liaohai Chen, Seok-Hwan Chung, Seth Darling, Haifeng Ding, Eric Fullerton, Marcos Grimsditch, Konstantin Guslienko, Axel Hoffmann, Yi Ji, Sam Jiang, Xiao-Min Lin, Val Novosad, John Pearson, and Andreas Scholl for their illuminating discussions of many facets of nanomagnetism. Thanks also to the hosts at the various institutions where this colloquium talk was presented. Finally, thanks to DARPA for partially supporting the magnetic virus research, and the University of Chicago–Argonne National Laboratory Consortium for Nanoscience Research.

REFERENCES

Abrikosov, A., 1957, Zh. Eksp. Teor. Fiz. **32**, 1442 [Sov. Phys. JETP **5**, 1174, 1957].
Aharoni, A., 1996, *Introduction to the Theory of Ferromagnetism* (Clarendon, Oxford).
AlHajDarwish, M., H. Kurt, S. Urazhdin, A. Fert, R. Loloee, W. P. Pratt, Jr., and J. Bass, 2004, Phys. Rev. Lett. **93**, 157203.
Alivisatos, A. P., 1996, Science **271**, 933.
Allen, M., D. Willits, J. Mosolf, M. Young, and T. Douglas, 2002, Adv. Mater. **14**, 1562.

Anders, S., H. A. Padmore, R. M. Duarte, T. Renner, T. Stammler, A. Scholl, M. R. Scheinfein, J. Stöhr, L. Séve, and B. Sinkovic, 1999, Rev. Sci. Instrum. **70**, 3973.
Baker, T. S., N. H. Olson, and S. D. Fuller, 1999, Microbiol. Mol. Biol. Rev. **63**, 862.
Bardeen, J., and W. H. Brattain, 1948, Phys. Rev. **74**, 230.
Bates, F. S., and G. H. Fredrickson, 1999, Phys. Today **52** (2), 32.
Bauer, G. E. W., A. Brataas, Y. Tserkovnyak, and B. J. van Wees, 2003, Appl. Phys. Lett. **82**, 3928.
Berger, L., 1996, Phys. Rev. B **54**, 9353.
Berkowitz, A. E., and Kentaro Takano, 1999, J. Magn. Magn. Mater. **200**, 552.
Bode, M., 2003, Rep. Prog. Phys. **66**, 523.
Buchanan, Kristen, K. Yu. Guslienko, A. Doran, A. Scholl, S. D. Bader, and V. Novosad, 2005, Phys. Rev. B **72**, 134415.
Buess, M., R. Höllinger, T. Haug, K. Perzlmaier, U. Krey, D. Pescia, M. R. Scheinfein, D. Weiss, and C. H. Back, 2004, Phys. Rev. Lett. **93**, 077207.
Cerritelli, M. E., N. Cheng, A. H. Rosenberg, C. E. McPherson, F. P. Booy, and A. C. Steven, 1997, Cell **91**, 271.
Chapman, S., 1944, Nature **154**, 132.
Cheng, J. Y., C. A. Ross, E. L. Thomas, H. I. Smith, and G. J. Vancso, 2003, Adv. Mater. **15**, 1599.
Chung, S. H., A. Hoffmann, S. D. Bader, L. Chen, C. Liu, B. Kay, and L. Makowski, 2004, Appl. Phys. Lett. **85**, 2971.
Coehoorn, R., D. B. de Mooij, and C. De Waard, 1989, J. Magn. Magn. Mater. **80**, 101.
Cowburn, R. P., and M. E. Welland, 2000, Science **287**, 1466.
Croat, J. J., J. F. Herbst, R. W. Lee, and F. E. Pinkerton, 1984, J. Appl. Phys. **55**, 2079.
Darling, S. B., and S. D. Bader, 2005, J. Mater. Chem. **15**, 4189.
Darling, S. B., N. A. Yufa, A. L. Cisse, S. D. Bader, and S. J. Sibener, 2005, Adv. Mater. (Weinheim, Ger.) **17**, 2446.
de Groot, R. A., F. M. Mueller, P. G. van Engen, and K. H. J. Buschow, 1983, Phys. Rev. Lett. **50**, 2024.
Ding, H. F., A. K. Schmid, Dongqi Li, K. Yu. Guslienko, and S. D. Bader, 2005, Phys. Rev. Lett. **94**, 157202.
DiVincenzo, D. P., and D. Loss, 1999, J. Magn. Magn. Mater. **200**, 271.
Douglas, T., and M. Young, 1998, Nature **393**, 152.
Elemans, J. A. A. W., A. E. Rowan, and R. J. M. Nolte, 2003, J. Mater. Chem. **13**, 2661.
Fitzsimmons, M. R., S. D. Bader, J. A. Borchers, G. P. Felcher, J. K. Furdyna, A. Hoffman, J. B. Kortright, I. K. Schuller, T. C. Schulthess, S. K. Sinha, M. F. Toney, D. Weller, and S. Wolf, 2004, J. Magn. Magn. Mater. **271**, 103.
Fullerton, E. E., J. S. Jiang, and S. D. Bader, 1999, J. Magn. Magn. Mater. **200**, 392.
Gider, S., D. D. Awschalom, T. Douglas, K. Wong, S. Mann, and G. Cain, 1996, J. Appl. Phys. **79**, 5324.
Gilbert, W., 1600, *De Magnete*.
Gilles, C., P. Bonville, K. K. W. Wong, and S. Mann, 2000, Eur. Phys. J. B **17**, 417.
Grimsditch, M., P. Vavassori, V. Novosad, V. Metlushko, H. Shima, Y. Otani, and K. Fukamichi, 2002, Phys. Rev. B **65**, 172419.
Guslienko, K. Yu, Kristen S. Buchanan, S. D. Bader, and V. Novosad, 2005, Appl. Phys. Lett. **86**, 223112.
Guslienko, K. Yu., V. Novosad, Y. Otani, H. Shima, and K. Fukamichi, 2001, Appl. Phys. Lett. **78**, 3848.
Hassoun, M. M., W. C. Black, Jr., E. K. F. Lee, R. L. Geiger, and A. Hurst, Jr., 1997, IEEE Trans. Magn. **33**, 3307.
Herbst, J. F., 1991, Rev. Mod. Phys. **63**, 819.
Hofer, W. A., A. S. Foster, and A. L. Shluger, 2003, Rev. Mod. Phys. **75**, 1287.
Hoffmann, A., S. H. Chung, S. D. Bader, L. Makowski, and L. Chen, 2006, in *Biomedical Applications of Nanotechnology*, edited by V. Labhasetwar and D. L. Leslie-Pelecky (Wiley, New York).
Hubert, A., and R. Schäfer, 1998, *Magnetic Domains* (Springer, Berlin).
Jedema, F. J., A. T. Filip, and B. J. Van Wees, 2001, Nature **410**, 345.
Jedema, F. J., H. B. Heersche, A. T. Filip J. J. A. Baselmans, and B. J. Van Wees, 2002, Nature **416**, 713.
Jeyadevan, B., K. Urakawa, A. Hobo, N. Chinnasamy, K. Shinoda, K. Tohji, D. D. J. Djayaprawira, M. Tsunoda, and M. Takahashi, 2003, Jpn. J. Appl. Phys., Part 2 **42**, L350.
Ji, Y., A. Hoffmann, J. S. Jiang, and S. D. Bader, 2004, Appl. Phys. Lett. **85**, 6218.
Jiang, J. S., S. D. Bader, H. Kaper, G. K. Leaf, R. D. Shull, A. J. Shapiro, V. S. Gornakov, V. I. Nikitenko, C. L. Platt, A. E. Berkowitz, S. David, and E. E. Fullerton, 2002, J. Phys. D **35**, 2339.
Jiang, J. S., A. Inomata, C.-Y. You, J. E. Pearson, and S. D. Bader, 2001, J. Appl. Phys. **89**, 6817.
Johnson, M., 1996, Nanotechnology **7**, 390.
Johnson, M., and R. H. Silsbee, 1985, Phys. Rev. Lett. **55**, 1790.
Katine, J. A., F. J. Albert, R. A. Buhrman, E. B. Myers, and D. C. Ralph, 2000, Phys. Rev. Lett. **84**, 3149.
Kilcoyne, S. H., and R. Cywinski, 1995, J. Magn. Magn. Mater. **140-144**, 1466.
Kimura, T., J. Hamrle, Y. Otani, K. Tsukagoshi, and Y. Aoyagi, 2004, Appl. Phys. Lett. **85**, 3501.
Kittel, C., 1996, *Introduction to Solid State Physics*, 7th ed. (Wiley, New York), p. 475.
Kneller, E. F., and R. Hawig, 1991, IEEE Trans. Magn. **27**, 3588.
Kortright, J. B., D. D. Awschalom, J. Stöhr, S. D. Bader, Y. U. Idzerda, S. S. P. Parkin, I. K. Schuller, and H.-C. Siegmann, 1999, J. Magn. Magn. Mater. **2**, 7.
Leuenberger, M. N., and D. Loss, 2001, Nature **410**, 789.
Lin, Y., A. Boker, J. He, K. Sill, H. Xiang, C. Abetz, X. Li, J. Wang, T. Emrick, S. Long, Q. Wang, A. Balazs, and T. P. Russell, 2005, Nature **434**, 55.
Liu, Chinmei, Seok-Hwan Chung, April Sutton, Funing Yan, Qiaoling Jin, A. Hoffmann, B. K. Kay, S. D. Bader, L. Makowski, and Liaohai Chen, 2005, J. Magn. Magn. Mater. (in press).
Luis, F., E. del Barco, J. M. Hernández, E. Remiro, J. Bartolomé, and J. Tejada, 1999, Phys. Rev. B **59**, 11837.
Mann, S., 1995, J. Mater. Chem. **5**, 935.
Mao, C., D. J. Solis, B. D. Reiss, S. T. Kottmann, R. Y. Sweeney, A. Hayhurst, G. Georgiou, B. Iverson, and A. M. Belcher, 2004, Science **303**, 213.
Martín, J. I., J. Nogués, K. Liu, J. L. Vicent, and I. K. Schuller, 2003, J. Magn. Magn. Mater. **256**, 449.
Matsuno, T., S. Sugahara, and M. Tanaka, 2004, Jpn. J. Appl. Phys., Part 1 **43**, 6032.
Meier, F., J. Levy, and D. Loss, 2003, Phys. Rev. Lett. **90**, 047901.
Mryasov, O. N., U. Nowak, K. Y. Guslienko, and R. W. Chantrell, 2005, Europhys. Lett. **69**, 805.
Murray, C. B., C. R. Kagan, and M. G. Bawendi, 1995, Science **270**, 1335.

Naito, K., H. Hieda, M. Sakurai, Y. Kamata, and K. Asakawa, 2002, IEEE Trans. Magn. **38**, 1949.
Nakamura, K., T. Ito, and A. J. Freeman, 2003, Phys. Rev. B **68**, 180404R.
Nikonov, D. E., and G. I. Bourianoff, 2005, IEEE Trans. Nanotechnol. **4**, 206.
Nogués, J., and I. K. Schuller, 1999, J. Magn. Magn. Mater. **192**, 203.
Novosad, V., M. Grimsditch, J. Darrouzet, J. Pearson, S. D. Bader, V. Metlushko, K. Guslienko, Y. Otani, H. Shima, and K. Fukamichi, 2003, Appl. Phys. Lett. **82**, 3716.
Novosad, V., K. Yu. Guslienko, H. Shima, Y. Otani, K. Fukamichi, N. Kikuchi, O. Kitakami, and Y. Shimada, 2001, IEEE Trans. Magn. **37**, 2088.
Novosad, V., K. Yu. Guslienko, H. Shima, Y. Otani, S. G. Kim, K. Fukamichi, N. Kikuchi, O. Kitakami, and Y. Shimada, 2002, Phys. Rev. B **65**, 060402(R).
Ohno, H., 1998, Science **281**, 951.
Okuno, T., K. Shigeto, T. Ono, K. Mibu, and T. Shinjo, 2002, J. Magn. Magn. Mater. **2**, 1.
Pankhurst, Q. A., J. Connolly, S. K. Jones, and J. Dobson, 2003, J. Phys. D **36**, R167.
Park, J. P., P. Eames, D. M. Engebretson, J. Berezovsky, and P. A. Crowell, 2003, Phys. Rev. B **67**, 020403(R).
Parkin, S., X. Jiang, C. Kaiser, A. Panchula, K. Roche, and M. Samant, 2003, Proc. IEEE **91**, 661.
Puntes, V. F., K. M. Krishnan, and A. P. Alivisatos, 2001, Science **291**, 2115.
Qiu, Z. Q., and S. D. Bader, 2000, Rev. Sci. Instrum. **71**, 1243.
Rosenberg, A., K. Griffin, F. W. Studier, M. McCormick, J. Berg, R. Novy, and R. Mierendorf, 1996, Novagen InNovations Newsletter, issue 6, p. 1, available at http://www.emdbiosciences.com/html/NVG/inNovations.html
Sagawa, M., S. Fujirama, H. Yamamoto, and K. Hiraga, 1984, IEEE Trans. Magn. **20**, 1584.
Samia, Anna C., K. Hyzer, J. Schlueter, J. S. Jiang, S. D. Bader, and X.-M. Lin, 2005, J. Am. Chem. Soc. **127**, 4126.
Sasaki, Y., M. Mizuno, A. C. C. Yu, T. Miyauchi, D. Hasegawa, T. Ogawa, M. Takahashi, B. Jeyadevan, K. Tohji, K. Sato, and S. Hisano, 2005, IEEE Trans. Magn. **41**, 660.
Skomski, R., and J. M. D. Coey, 1993, Phys. Rev. B **48**, 15812.
Slonczewski, J. C., 1996, J. Magn. Magn. Mater. **159**, L1.
Stöhr, J., 1999, J. Magn. Magn. Mater. **200**, 470.
Sugahara, S., and M. Tanaka, 2004, Appl. Phys. Lett. **84**, 2307.
Sun, S., C. B. Murray, D. Weller, L. Folks, and A. Moser, 2000, Science **287**, 1989.
Tehrani, S., J. M. Slaughter, M. DeHerrera, B. Engel, N. D. Rizzo, J. Salter, J. Durlam, R. W. Dave, J. Janesky, B. Butcher, K. Smith, and G. Grynkewich, 2003, Proc. IEEE **91**, 703.
Teng, X., and H. Yang, 2003, J. Am. Chem. Soc. **125**, 14559.
Valenzuela, S. O., and M. Tinkham, 2004, Appl. Phys. Lett. **85**, 5914.
Vavassori, P., N. Zaluzec, V. Metlushko, V. Novosad, B. Ilic, and M. Grimsditch, 2004, Phys. Rev. B **69**, 214404.
Weller, D., and A. Moser, 1999, IEEE Trans. Magn. **35**, 4423.
Weller, D., A. Moser, L. Folks, M. E. Best, W. Lee, M. F. Toney, M. Schwickert, J.-U. Thiele, and M. F. Doerner, 2000, IEEE Trans. Magn. **36**, 10.
Wernsdorfer, W., N. Aliga-Alcalde, D. N. Hendrickson, and G. Christou, 2002, Nature **416**, 406.
Whitesides, G. M., and B. Grzybowski, 2002, Science **295**, 2418.
Wolf, S. A., D. D. Awschalom, R. A. Buhrman, J. M. Daughton, S. von Molnár, M. L. Roukes, A. Y. Chtchelkanova, and D. M. Trege, 2001, Science **294**, 1488.
Xiong, Z. H., D. Wu, Z. V. Vardeny, and J. Shi, 2004, Nature **427**, 821.
Zeng, H., J. Li, J. P. Liu, Z. L. Wang, and S. Sun, 2002, Nature **420**, 395.
Zhang, S., 2003, Nat. Biotechnol. **21**, 1171.
Zutic I., J. Fabian, and S. Das Sarma, 2004, Rev. Mod. Phys. **76**, 323.